

Rice Mitogen-Activated Protein Kinase Interactome Analysis Using the Yeast Two-Hybrid System^{1[C][W]}

Raksha Singh, Mi-Ok Lee, Jae-Eun Lee, Jihyun Choi, Ji Hun Park, Eun Hye Kim, Ran Hee Yoo, Jung-Il Cho, Jong-Seong Jeon, Randeep Rakwal, Ganesh Kumar Agrawal, Jae Sun Moon, and Nam-Soo Jwa*

Department of Molecular Biology, College of Life Sciences, Sejong University, Gunja-dong, Gwangjin-gu, Seoul 143-747, Republic of Korea (R.S., M.-O.L., J.-E.L., J.C., J.H.P., E.H.K., N.-S.J.); Plant Systems Engineering Center, Korea Research Institute of Bioscience and Biotechnology, Daejeon 305-333, Republic of Korea (R.H.Y., J.S.M.); Biosystems and Bioengineering Program, University of Science and Technology, Yuseong-gu, Daejeon 305-350, Republic of Korea (R.H.Y., J.S.M.); Graduate School of Biotechnology and Crop Biotech Institute, Kyung Hee University, Yongin 446-701, Republic of Korea (J.-I.C., J.-S.J.); Graduate School of Life and Environmental Sciences, University of Tsukuba, Tsukuba, Ibaraki 305-8572, Japan (R.R.); Department of Anatomy I, Showa University School of Medicine, Shinagawa, Tokyo 142-8555, Japan (R.R.); and Research Laboratory for Biotechnology and Biochemistry, Kathmandu 44600, Nepal (R.R., G.K.A.)

Mitogen-activated protein kinase (MAPK) cascades support the flow of extracellular signals to intracellular target molecules and ultimately drive a diverse array of physiological functions in cells, tissues, and organisms by interacting with other proteins. Yet, our knowledge of the global physical MAPK interactome in plants remains largely fragmented. Here, we utilized the yeast two-hybrid system and coimmunoprecipitation, pull-down, bimolecular fluorescence complementation, subcellular localization, and kinase assay experiments in the model crop rice (*Oryza sativa*) to systematically map what is to our knowledge the first plant MAPK-interacting proteins. We identified 80 nonredundant interacting protein pairs (74 nonredundant interactors) for rice MAPKs and elucidated the novel proteome-wide network of MAPK interactors. The established interactome contains four membrane-associated proteins, seven MAP2Ks (for MAPK kinase), four MAPKs, and 59 putative substrates, including 18 transcription factors. Several interactors were also validated by experimental approaches (in vivo and in vitro) and literature survey. Our results highlight the importance of OsMPK1, an ortholog of tobacco (*Nicotiana benthamiana*) salicylic acid-induced protein kinase and Arabidopsis (*Arabidopsis thaliana*) AtMPK6, among the rice MAPKs, as it alone interacts with 41 unique proteins (51.2% of the mapped MAPK interaction network). Additionally, Gene Ontology classification of interacting proteins into 34 functional categories suggested MAPK participation in diverse physiological functions. Together, the results obtained essentially enhance our knowledge of the MAPK-interacting protein network and provide a valuable research resource for developing a nearly complete map of the rice MAPK interactome.

Mitogen-activated protein kinases (MAPKs) play central roles in the signaling network as terminal components of MAPK cascades, which are composed of at least three sequentially activated MAPK family modules (MAP3Ks [for MAPK kinase kinase], MAP2Ks [for MAPK kinase], and MAPKs; Widmann et al., 1999;

Rodriguez et al., 2010). MAPK cascades are universal and highly conserved signal transduction modules among eukaryotes, including plants, which transduce extracellular signals intracellularly and determine the specificity of targets and responses (Widmann et al., 1999; Chang and Karin, 2001; Agrawal et al., 2003b; Hamel et al., 2006; Andreasson and Ellis, 2010; Rodriguez et al., 2010). Like other eukaryotic MAPKs, plant MAPKs have been shown to regulate a diverse array of cellular and physiological functions, including responses to multiple stressors and hormones, camalexin production, stomatal patterning and closure, ovule development, floral organ abscission, anther development, and leaf senescence (Agrawal et al., 2003a; Fiil et al., 2009; Pitzschke et al., 2009; Andreasson and Ellis, 2010; Rodriguez et al., 2010). Studies have also delineated a few MAPK cascades in plants (Pitzschke et al., 2009; Andreasson and Ellis, 2010; Rodriguez et al., 2010). One early example is the perception of a bacterial flagellin in Arabidopsis (*Arabidopsis thaliana*) by a signaling cascade composed of a Leu-rich repeat receptor

¹ This work was supported by the National Research Foundation of Korea (grant no. 2011-0000139), funded by the Korean government, and by the Next-Generation BioGreen 21 Program (Plant Molecular Breeding Center grant no. PJ007993) of the Rural Development Administration, Republic of Korea.

* Corresponding author; e-mail nsjwa@sejong.ac.kr.

The author responsible for distribution of materials integral to the findings presented in this article in accordance with the policy described in the Instructions for Authors (www.plantphysiol.org) is: Nam-Soo Jwa (nsjwa@sejong.ac.kr).

[C] Some figures in this article are displayed in color online but in black and white in the print edition.

[W] The online version of this article contains Web-only data.
www.plantphysiol.org/cgi/doi/10.1104/pp.112.200071

kinase, MEKK1 (a MAP3K), MKK4/MKK5 (MAP2Ks), MPK3/MPK6 (MAPKs), and WRKY22/WRKY29 (transcription factors [TFs]; Asai et al., 2002).

Tremendous progress in elucidating the physiological responses of plant MAPKs is the outcome of numerous studies conducted in recent decades. Nonetheless, little is known about MAPKs' specific upstream activators and downstream targets. Despite these gaps in our knowledge, it is clear that the MAPK cascade is embedded in a rich network of interactions with a wide variety of other components, including membrane receptors, TFs, kinase scaffolds, activators, and repressors. Consequently, researchers have been advocating a system-level approach to map these additional components and to elucidate their MAPK-related functions (Kolch et al., 2005; Blüthgen and Legewie, 2008).

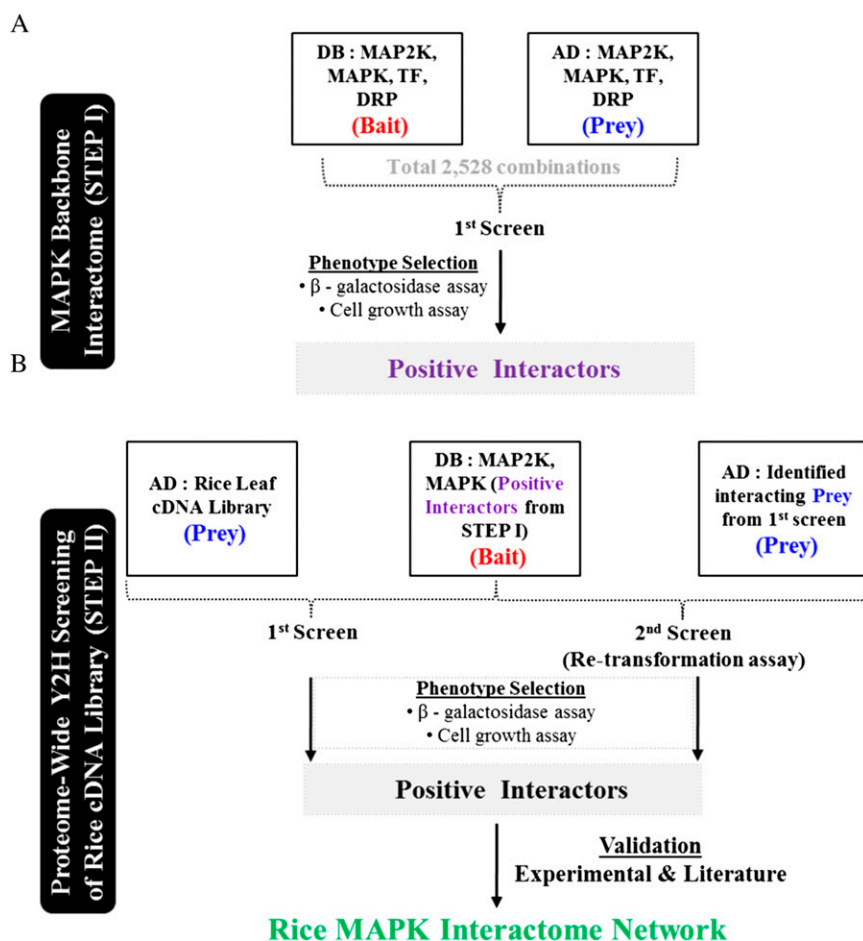
Two high-throughput protein microarray studies and one comprehensive study have been performed in Arabidopsis to identify the MAPK substrates (Feilner et al., 2005; Lee et al., 2008a; Popescu et al., 2009). The Arabidopsis genome encodes approximately 60 MAP3Ks, 10 MAP2Ks, and 20 MAPKs (Ichimura et al., 2002). Feilner et al. (2005) identified 48 and 39 potential phosphorylation substrates of AtMPK3 and AtMPK6, respectively, while Popescu et al. (2009) identified 570

MAPK phosphorylation substrates (Feilner et al., 2005; Popescu et al., 2009). Recently, the Arabidopsis Interactome Mapping Consortium (2011) constructed an Arabidopsis interactome map containing 6,200 highly reliable protein-protein interactions (PPIs; Arabidopsis Interactome Mapping Consortium, 2011). Apart from these studies, no system-level analyses, including the yeast two-hybrid (Y2H) approach, have been undertaken to elucidate the comprehensive MAPK interactome in either Arabidopsis or other sequenced plants, including the monocot model crop rice (*Oryza sativa*; Agrawal and Rakwal, 2006, 2011; Feuillet et al., 2011). As PPIs are vital for almost all biological functions, a systematic high-throughput survey of physical interactions between MAPKs and the rest of the proteome is one way to address the challenging task of identifying upstream and downstream signaling components of MAPK cascades at the global level (Morsy et al., 2008).

Here, we applied the most frequently used Y2H binary approach to detect interacting proteins in rice in a high-throughput manner to construct a proteome-wide rice MAPK interaction network. Comparable to Arabidopsis, the rice genome is predicted to encode 75 MAP3Ks, eight MAP2Ks, and 17 MAPKs (Agrawal et al., 2003b; Hamel et al., 2006; Reyna and Yang, 2006;

Figure 1. Experimental strategy for establishing a proteome-wide rice MAPK interactome.

A, Backbone construction of a MAPK interactome. Rice full-length cDNAs (MAP2K, MAPK, TF, and DRP) in DB and AD vectors were subjected to 2,528 possible combinatorial cross-interactions. Positive interacting protein pairs derived from the first screening gave rise to a MAPK backbone interactome. B, Proteome-wide screening of the rice MAPK interactome. Rice MAPKs and MAP2Ks identified in the backbone interactome were used as baits, and the rice leaf cDNA library was used as prey. Positive interactions from the first screen were confirmed by the retransformation assay in the second screen. Positive interactors from the first and second screens were used to develop a rice MAPK interactome. [See online article for color version of this figure.]



Rao et al., 2010). The experimental strategies involved in this study include the following: (1) screening for physical interactions between MAPKs and the rice complementary DNA (cDNA) library; (2) validation of identified interactors by in vivo and in vitro approaches (including coimmunoprecipitation [Co-IP], cellular localization studies, and kinase assays) and literature-based survey; and (3) construction and functional interpretation of the MAPK Y2H network. These combined approaches enabled us to establish the rice MAPK interaction network composed of 74 nonredundant (NR) interactors, which highlights the importance of OsMPK1, an ortholog of the well-studied tobacco (*Nicotiana benthamiana*) SIPK and Arabidopsis AtMPK6, in physiological functions.

RESULTS

Mapping a Rice MAPK Interaction Network

A two-stage Y2H screening system was used as an experimental strategy to identify rice MAPK-interacting proteins (Fig. 1A). In the first stage (primary Y2H screen), we used 53 rice MAPK-related bait proteins (nine MAPKs, nine MAP2Ks, 25 TFs, and 10 defense-responsive proteins [DRPs]; Supplemental Table S1) and performed a total of 2,528 possible cross-interactions including

empty vector to exclude potential autoactivators (Supplemental Fig. S1). One of the nine MAP2Ks, OsWNK1, does not contain Lys residues but belongs to the MAP2K family protein (Kim et al., 2000). Therefore, we also included OsWNK1 in the MAP2K group. The selected MAPKs cover all phylogenetic groups (Reyna and Yang, 2006). This initial screen yielded 13 NR interacting protein pairs (IPPs; 13 NR interactors) showing growth on synthetic complete lacking Leu-Trp (SC-LT; +5 mM 3-amino-1,2,4-triazole [3-AT]) plates (Supplemental Table S1; for details, see “Materials and Methods”). The 13 interactors were composed of two MAPKs (OsMPK1 and OsMPK8), five MAP2Ks (OsMEK1, OsMEK2, OsMEK7b, OsMEK8a, and OsWNK1), and six TFs (OsWRKY51, OsbZIP50, OsbZIP46, OsNPR1, OsNPR1-like, and OsTGA3). This small set of interactors provided a backbone MAPK interactome for systematic proteome-wide screening of MAPK interactors in rice.

In the second stage, the MAPKs and MAP2Ks in the backbone interactome plus two MAPKs, OsMPK5 and OsMPK6, were used as bait proteins for a proteome-wide Y2H screen of the rice leaf cDNA library (Fig. 1B; for details, see “Materials and Methods”). The number of diploids screened and the number of prey identified for each bait are given in Supplemental Table S2. A total of 71 NR IPPs and 63 NR interactors

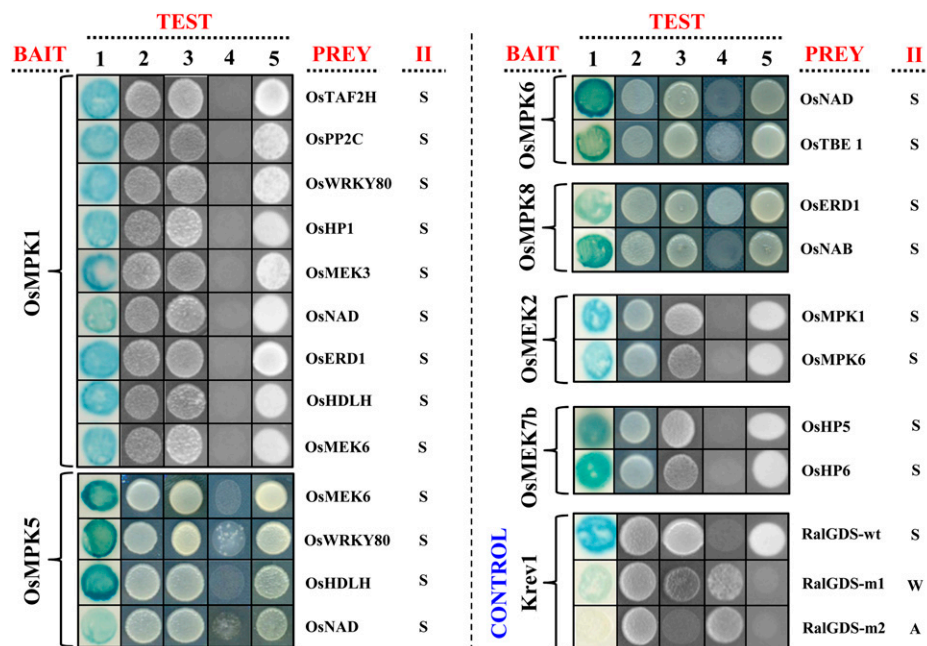


Figure 2. Genome-wide Y2H screening of the rice MAPK interactors using the rice cDNA library. Results for some of the PPIs are provided as examples. Five tests (lanes 1–5) used to determine the PPIs were the β -galactosidase assay (lane 1) and cell growth on various solid selection media (SC-LT [lane 2], SC-LT + 25 mM 3-AT [lane 3], SC-LT + 0.2% 5-FOA [lane 4], and SC-LTU [lane 5]). Control tests were performed to assign the qualitative interaction intensity (II) for other interacting protein pairs. Control plasmid pairs are as follows: S (strong), pEXP32/Krev1 + pEXP22/RaIGDS-wt; W (weak), pEXP32/Krev1 + pEXP22/RaIGDS-m1; A (absent), pEXP32/Krev1 + pEXP22/RaIGDS-m2. Krev1 (Rap1A) is a member of the Ras family of GTP-binding proteins. RaIGDS is RaL guanine nucleotide dissociation stimulator protein, and its mutants are RaIGDS-m1 and RaIGDS-m2. Details of all identified MAPK-interacting proteins are provided in Supplemental Table S3. [See online article for color version of this figure.]

were identified (Supplemental Table S3). OsMPK1, OsMPK5, OsMPK6, and OsMPK8 were found to interact with 37, 10, five, and seven potential NR interactors, respectively (Supplemental Table S3). For MAP2Ks, two NR interactors were identified each for OsMEK1, OsMEK2, and OsMEK7b, and four NR interactors were identified for OsWINK1 (Supplemental Table S3). We did not find any interacting partner for OsMEK8a by library screening. A retransformation assay confirmed all the identified interactors to be positive interactors, excluding technical false positives (Fig. 1B; for details, see “Materials and Methods”). All screened positive interactors (63) were checked for the presence of an “in-frame” Gal4 activation domain (AD) fusion. The size of the positive interactors varied from approximately 500 to 2,000 bp, as shown by the sequencing data (Macrogen). We differentiated the interaction intensity between the interacting pairs, as interaction specificity is a critical issue in MAPK signaling (Bardwell, 2006). Forty-seven IPPs indicated strong interaction intensity by showing growth on various selection media (SC-LT, synthetic complete lacking Leu-Trp-His [SC-LTH; +25 mM 3-AT], SC-LT + 0.2% 5-fluoroorotic acid [5-FOA], and synthetic complete lacking Leu-Trp-uracil [SC-LTU]) and blue color in a β -galactosidase assay within 2 to 4 d, whereas 33 IPPs were considered as weak interactors as they needed longer incubation times for growth and color change. The Y2H results for some of the strong IPPs are shown as representative examples in Figure 2. Autoactivated PPIs were found for three IPPs (OsMPK1/OsPRO, OsMPK1/OsAP, and OsMPK5/OsAP1) in a retransformation assay and were not counted as valid PPIs (Supplemental Tables S2 and S3). Library screening and creation of the backbone interactome together resulted in the identification of 80 NR IPPs and 74 NR interactors (Table I; Supplemental Table S3). Gene Ontology annotation using The Rice

Genome Annotation Project Database revealed their possible involvement in diverse molecular and biological processes encompassing 34 functional categories and significant enrichment of proteins involved in stress responses (Supplemental Fig. S2; Supplemental Table S3). As mentioned below, subsets of IPPs were validated using in vivo, in vitro, and literature survey approaches, providing evidence that the established rice MAPK interactome is of high quality.

Validation of the Interactome by in Vivo Co-IP and in Vitro Glutathione S-Transferase Pull-Down Assays

Among 15 identified IPPs tested, only 10 IPPs (six MAPKs/MAP2Ks and four MAPKs/TFs) were efficiently expressed in BL21 cells as glutathione S-transferase (GST) and His tag recombinant proteins. Out of 10 IPPs, only two IPPs were expressed in tobacco as a he-magglutinin (HA), Myc, or His tag recombinant protein. We could not express other proteins either in BL21 or in tobacco under our laboratory conditions. Thus, the expressed proteins were subjected to in vivo/in vitro assays to assess their interactions. Of the MAPKs, OsMPK1 and OsMPK6 were used, as they interact with a number of proteins (Supplemental Table S3) and their plant orthologs (such as AtMPK6 and AtMPK4 in Arabidopsis) have been well studied (Andreasson and Ellis, 2010). In vivo Co-IP was performed with two IPPs (Myc:OsMPK1/HA:OsMEK2 and His:OsMPK6/Myc:OsMEK2), as they were expressed transiently in tobacco cells (Fig. 3A). Before performing the Co-IP, the protein expression was checked (Fig. 3, A and B), then the cell lysates were used for Co-IP by HA antibody and immunoblotted with Myc antibody as shown in Figure 3A. In Figure 3B, cell lysates were immunoprecipitated with Myc antibody and immunoblotted with

Table I. Summary of rice MAPK interactome

HP, Hypothetical protein; ME, metabolic enzyme, N/D, not detected; RE, regulatory enzyme.

Protein Family	Y2H Baits	MAPK	Kinase	TF	HP	RE	ME	Total Interactors	Total Interactome	In Vivo Validation				In Vitro Validation		Literature Validation			
										Co-IP	BiFC		Subcellular Localization	GST Pull Down	Kinase Assay	Rice	Arabidopsis	Yeast	Human
											Rice	Onion							
MAPK	OsMPK1	6		9	5	10	11	42	41	1	3	4	8	9	2	2	7	1	1
	OsMPK3											N/D							
	OsMPK4											N/D							
	OsMPK5	1		2	1	4	2	11	10				2			3	1		
	OsMPK6						2	3	5	1	1	1	2	1			2	1	
	OsMPK8	1		4	3	1	1	11	10				3		1	2			
	OsMPK9											N/D							
	OsMPK11											N/D							
	OsMPK15											N/D							
MAP2K	OsMEK1	2						3	2				2	1		1	1		
	OsMEK2	2						3	2	2	2	2	2	2	1		2	2	1
	OsMEK3	1						2	1				1	1	1		1		
	OsMEK6	2						3	2				2			2	2		
	OsMEK7a											N/D							
	OsMEK7b	2				2		5	4				2	1			1		
	OsMEK8a	1						2	1				1	1			1		
	OsMEK8b											N/D							
	OsWINK1	2	1	1		1	2	8	7				2		1		1		

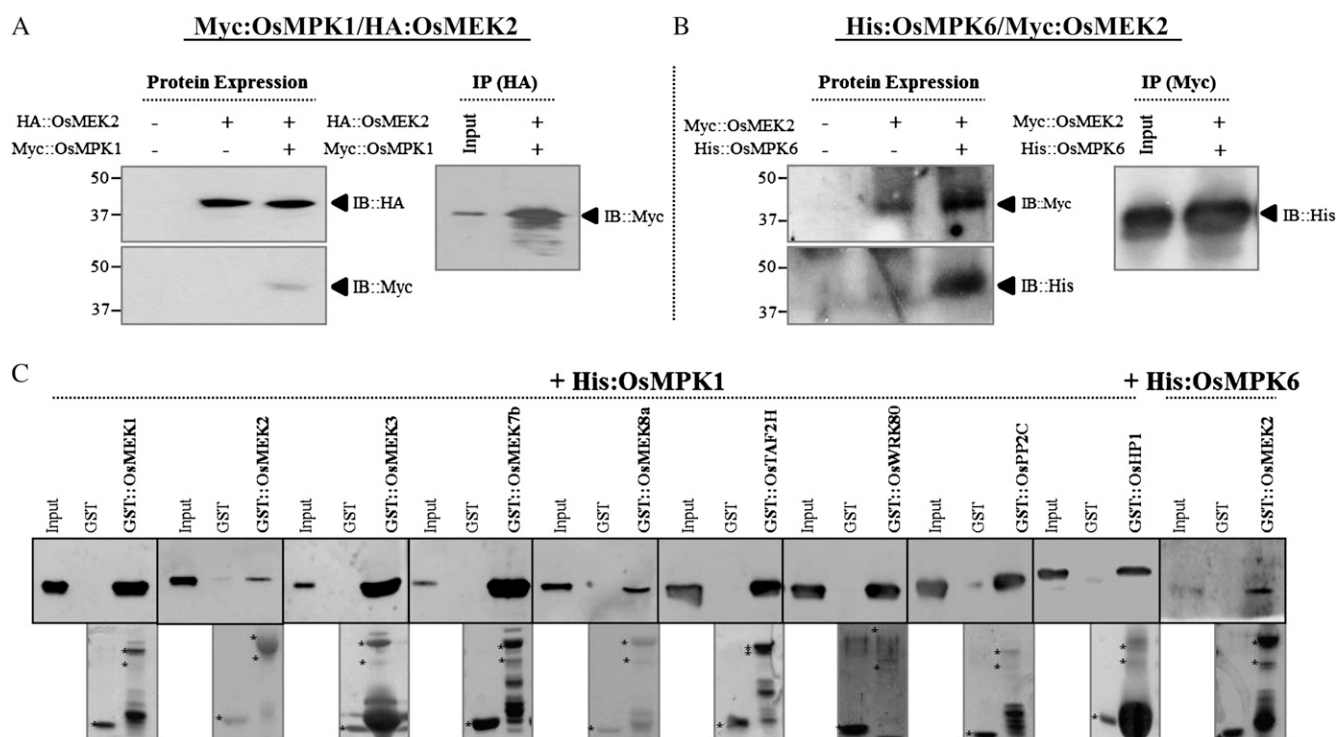


Figure 3. Validation of the Y2H-based identified IPPs by Co-IP and GST pull-down assays. A, Immunoblotting of Co-IP sample using Myc and HA antibodies. In vivo Co-IP was performed using tobacco leaves infiltrated with *Agrobacterium* C58C1 strain harboring the desired interacting pair (Myc:OsMPK1/HA:OsMEK2). B, Immunoblotting of Co-IP sample using Myc and His antibodies. In vivo Co-IP was performed using tobacco leaves infiltrated with *Agrobacterium* C58C1 strain harboring the desired interacting pair (His:OsMPK6/Myc:OsMEK2). Symbols represent the presence (+) or absence (–) of the various proteins. C, In vitro GST pull-down assays for 10 interacting pairs. The top panel shows immunoblot analysis of the binding of His-bait fusion proteins (OsMPK1 and OsMPK6) to GST-prey fusion proteins or GST alone (control) using His antibody. Asterisks in the bottom panel indicate the *E. coli* expression of GST alone (control) and complexes of GST-prey with His-bait fusion proteins purified on columns of Glutathione-Sepharose 4B beads and nickel-nitrilotriacetic acid agarose chelating agarose CL-6B beads, respectively, and subsequently analyzed by SDS-PAGE and Coomassie Brilliant Blue staining. Input in A, B, and C was bait fusion protein. IB, Immunoblotting.

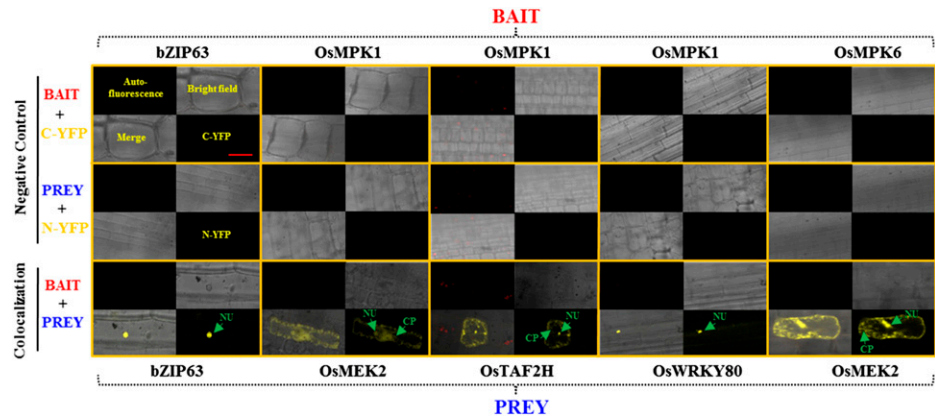
His antibody. In vitro GST pull-down assays were carried out for 10 IPPs, including His:OsMPK1/GST:OsMEK2 and His:OsMPK6/GST:OsMEK2. For all 10 IPPs, protein bands of the expected size were confirmed by Coomassie Brilliant Blue staining as shown (Fig. 3C, bottom panel). Figure 3C shows that the recombinant proteins His:OsMPK1 and His:OsMPK6 specifically interact with GST prey only (as indicated in lane 3) but not with GST alone (lane 2). These results further indicated that the tested IPPs interact physically.

Validation of the Interactome by in Vivo Bimolecular Fluorescence Complementation Assays in Rice Leaf Sheath and Onion Epidermal Cells

We applied the bimolecular fluorescence complementation (BiFC) approach to subsets of identified IPPs to assess whether the observed Y2H PPIs occur in living plant tissues/cells. The BiFC system is based on the formation of fluorescent complexes through the interaction of two proteins fused to nonfluorescent fragments of yellow fluorescent protein (YFP), which

yields a fluorescent YFP signal (Hu and Kerppola, 2003; Walter et al., 2004). Eight IPPs in the interactome were subjected to BiFC analysis in rice leaf sheath along with the Arabidopsis bZIP63 protein as a positive control (Fig. 4). bZIP63 reportedly forms homodimers and heterodimers, and when used as a positive control in the BiFC assay in Arabidopsis it is localized to the nucleus (Sibéril et al., 2001; Walter et al., 2004). As expected, bZIP63 gave a fluorescence signal and was localized to the nucleus. Out of eight IPPs checked, only four IPPs (OsMPK1/OsMEK2, OsMPK1/OsTAF2H, OsMPK1/OsWRKY80, and OsMPK6/OsMEK2) were detected (by fluorescence) in rice leaf sheath (Fig. 4; colocalization). But the remaining four IPPs failed to express efficiently in rice leaf sheath. The IPPs were also localized to the nucleus; however, with the exception of OsMPK1/OsWRKY80, the other three gave fluorescence signals throughout the tissue. The fluorescence signals for these IPPs were also observed in epidermal cells from onion (*Allium cepa*) along with one more identified IPP, OsMPK1/OsPP2C (Supplemental Fig. S3). For both rice and onion, we also tested the interaction

Figure 4. In vivo BiFC analysis of identified IPPs in rice leaf sheaths. Rice leaf sheath was transformed with mixtures of interacting protein pairs using a biolistic method as described in “Materials and Methods.” IPP bait and prey proteins were fused to the N- and C-terminal halves of YFP, respectively. YFP fluorescence and localization were observed by confocal laser microscopy. See text for details. CP, Cytoplasm; NU, nucleus. Bar = 5 μm. [See online article for color version of this figure.]



of each protein with negative control BiFC vectors carrying half of the YFP to detect false-positive interactions (Fig. 4; Supplemental Fig. S3; negative controls). No fluorescence signal was observed with any negative controls. These BiFC results thus indicate that the tested IPPs are genuine interacting pairs that interact in living rice tissue and onion cells.

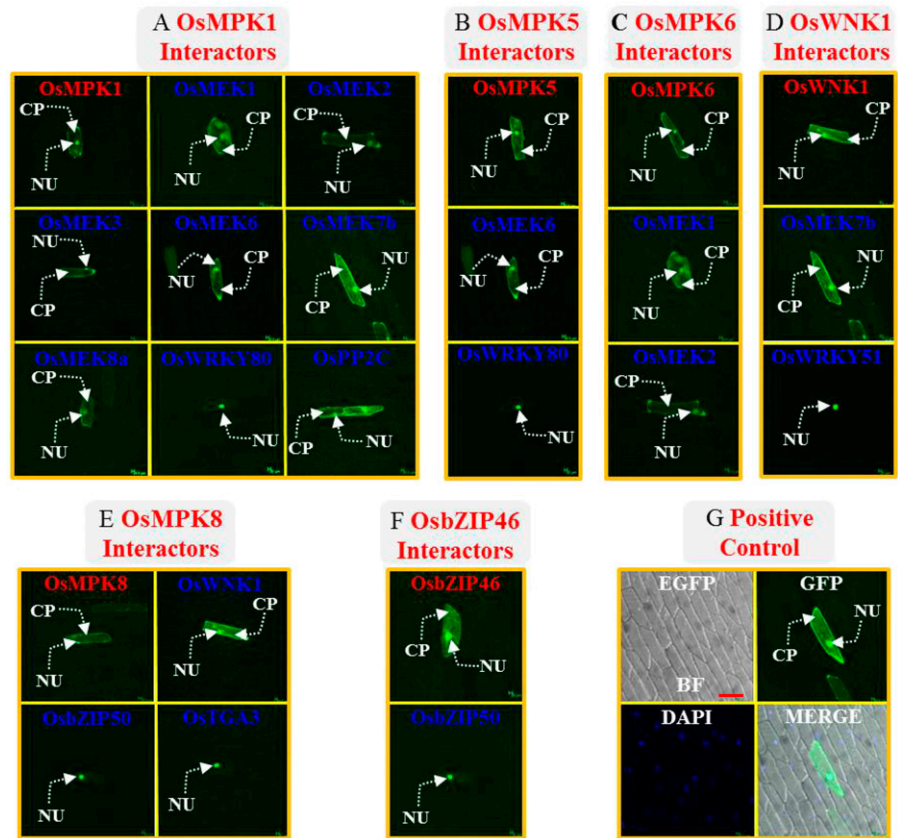
In Vivo Subcellular Localization of Identified IPPs Validates Their Biological Relevance

For biologically applicable PPIs, the interacting proteins generally colocalize to the same space or an interactable

subcellular space (Gandhi et al., 2006). Consequently, we tested the subcellular localization of 24 interactors, together involved in 18 IPPs in the interactome, along with GFP (positive control) by transiently expressing them as GFP fusion proteins in living onion cells (Fig. 5). GFP alone was localized to the nucleus and cytoplasm (Fig. 5G), as reported previously, suggesting that the localization system can be used to determine the locations of proteins of interest (Karimi et al., 2002; Lee et al., 2008b).

The OsMPK1 protein was localized to the nucleus and cytoplasm, and its interactors OsMEK1, OsMEK2, OsMEK3, OsMEK6, OsMEK7b, OsMEK8a, and OsPP2C,

Figure 5. Subcellular localization of individual interactors in onion epidermal cells. A, Subcellular localization analysis of OsMPK1 and its eight interacting partner proteins shows the presence of both bait and prey in the cytoplasm and nucleus except OsWRKY80, which was found to be localized only to the nucleus. B to F, Subcellular localization of OsMPK5 (B), OsMPK6 (C), OsWNK1 (D), OsMPK8 (E), and OsbZIP46 (F). G, GFP is shown as a positive control. CP, Cytoplasm; NU, nucleus. Bar = 20 μm. [See online article for color version of this figure.]



but not OsWRKY80, were localized to the same location (Fig. 5A). OsMPK5, OsWINK1, OsMPK8, OsMPK6, and OsbZIP46 were also localized to the nucleus and cytoplasm. Their interactors had the same location, except for the interacting TFs OsWRKY80, OsWRKY51, OsbZIP50, and OsTGA3 (Fig. 5, B–F). The KOME (for Knowledge-based *Oryza* Molecular biological Encyclopedia) Web site (http://cdna01.dna.affrc.go.jp/cDNA/CDNA_main_front.html) also reported the localization of these TFs in the nucleus. Reports suggest that even when both interacting proteins do not localize to the same cellular organelle, it is possible for one of them to translocate to the cellular organelle occupied by the other under certain physiological conditions (Samaj et al., 2002; Ahlfors et al., 2004; Lee et al., 2004; Shaffer et al., 2005). A growing body of evidence suggests that the cytoplasm-localized MAPKs and MAP2Ks interact with nucleus-localized TFs after translocation to the nucleus (Ligterink et al., 1997; Khokhlatchev et al., 1998). Hence, MAPKs and MAP2Ks potentially shuttle between the cytoplasm and nucleus, depending on their interactions (Lee et al., 2004).

We obtained localization information for all 74 interactors from the KOME Web site (Supplemental Table S3). Comparison of our experimental data for 18 IPPs (17 interactors) with the KOME data (Supplemental Table S3) revealed 88.2% identity (15 interactors), indicating that the KOME data are of high quality and suitable for large-scale comparative analysis. According to KOME localization information (Supplemental Table S3), out of the remaining 62 IPPs, each of 21 IPPs (26 interactors) colocalize. A high percentage of the 74 interactors were predicted to localize to the cytoplasm (29.7%) and the nucleus (28.3%). Other subcellular

locations included the chloroplast (13.5%), mitochondria (9.4%), endoplasmic reticulum (6.7%), microbody (6.7%), plasma membrane (4%), and outside (1.3%). These results further indicate that the established rice MAPK interactome is of high quality.

MAPKs Show Myelin Basic Protein Kinase Activity and Cophosphorylate Their MAPK Interactors

MAPKs regulate relevant signaling pathways by phosphorylating upstream and downstream substrates (Chen et al., 2001). We tested the myelin basic protein (MBP) kinase activity of two MAPKs (OsMPK1 and OsMPK6) and three MAP2Ks (OsMEK2, OsMEK3, and OsWINK1) and the cophosphorylation of MBP artificial substrate by three IPPs (OsMPK1/OsMEK2, OsMPK1/OsMEK3 and OsMPK8/OsWINK1) in an in vitro phosphorylation assay (Supplemental Fig. S4; Supplemental Table S3). All tested MAPKs and MAP2Ks showed strong MBP kinase activities (Supplemental Fig. S4A). Moreover, cophosphorylation activity was detected when OsMPK1 was incubated with OsMEK2 or OsMEK3 and OsMPK8 with OsWINK1 (Supplemental Fig. S4B) along with MBP. The band intensity for OsMPK8/OsWINK1 was stronger than those for OsMPK1/OsMEK2 and OsMPK1/OsMEK3. The band intensities for OsMPK1/OsMEK2 and OsMPK1/OsMEK3 IPPs were very weak (Supplemental Fig. S4B) relative to their individual MBP kinase activities, suggesting suppression of their phosphorylation activity as a result of the interactions (Supplemental Fig. S4A). Phosphorylation of MAP2Ks has previously been shown to suppress their kinase activity strongly in various eukaryotes (Xing et al.,

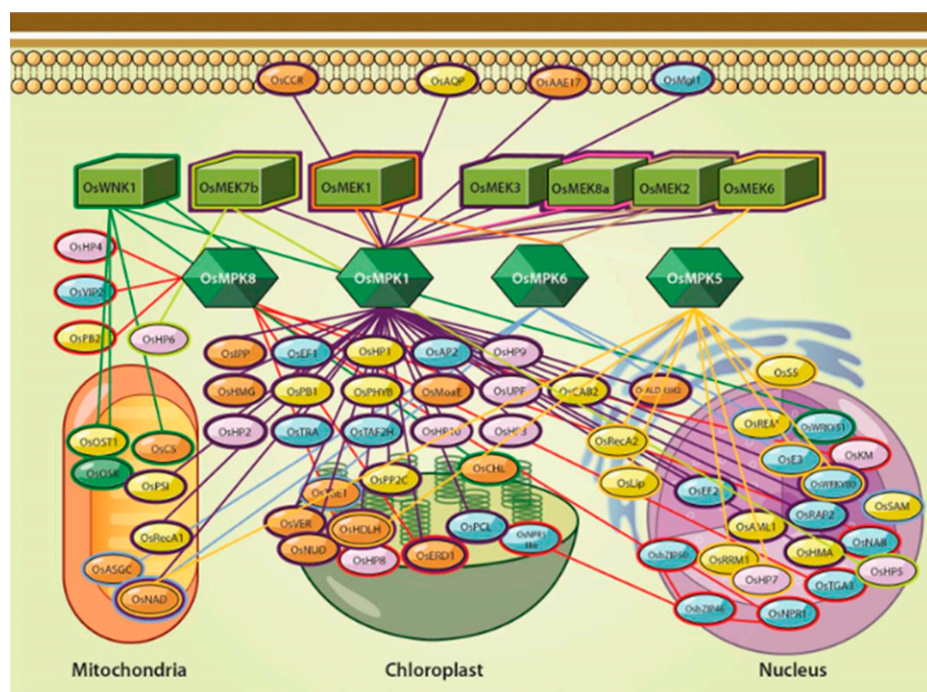


Figure 6. The rice MAPK interactome. The 80 PPIs for MAPK signaling components detected by Y2H screens are shown as an interaction network. Proteins are shown as cubes, hexagons, and circles, and interactions are shown as lines. The interaction pairs for each bait protein are separated by lines of different colors. Kinases are shown as light green and green cubes, hexagons, and circles. TF, regulatory enzyme (RE), metabolic enzyme (ME), and hypothetical protein (HP) are shown in blue, yellow, brown, and purple, respectively. Localization of all of the interacting proteins based on prediction and experimental data are shown. Details of all interaction pairs are given in Supplemental Table S3. [See online article for color version of this figure.]

2001; Yang et al., 2001; Gopalbhai et al., 2003). Hence, interacting MAPK pairs appear to control phosphorylation activity to inhibit or activate signaling pathways. These findings suggest that MAPKs and MAP2Ks are potential functional components of both a MAPK module and the interactome and that they regulate signaling pathways through phosphorylation of their interacting protein substrates.

Literature Validation of the Rice MAPK Interactome

The interactome components were subjected to literature validation across rice, Arabidopsis, yeast, and human (*Homo sapiens*; Supplemental Fig. S5; Supplemental Table S4) as per the National Center for Biotechnology Information search engine (<http://www.ncbi.nlm.nih.gov>). Of 80 NR IPPs, 21 (24 NR interactors) have been described in these four organisms (Supplemental Fig. S5). Arabidopsis alone accounted for 17 IPPs, with a few IPPs also being reported from yeast and/or human studies, such as OsMPK1/OsMEK1 and OsMPK1/OsMEK2 (Bardwell et al., 1996, 2001). When these 21 IPPs were compared with 20 experimentally supported IPPs (out of 80 IPPs), 11 IPPs (12 NR interactors) were found to be common in both analyses (Supplemental Figs. S5 and S6). Of 11 IPPs, the biological functions of 10 have been reported using multiple approaches (Supplemental Table S4). For example, OsMPK1 and its interactions with OsMEK1, OsMEK2, OsMEK6, OsMEK7b, OsMEK8a, and OsPP2C have been shown to be involved in growth, development,

and biotic and abiotic signaling and responses (see refs. in Supplemental Table S4). The 10 IPPs unique to the literature validation approach were OsMPK1/OsEF1, OsMPK1/OsPCL, OsMPK1/OsEF2, OsMPK5/OsNAD, OsMPK5/OsHP7, OsMPK8/OsHP4, OsMPK8/OsPB2, OsWNK1/OsOSR, OsbZIP46/OsNPR1-like, and OsbZIP46/OsNPR1 (Supplemental Figs. S5 and S6). Of these, OsbZIP46/OsNPR1-like and OsbZIP46/OsNPR1 are implicated in defense signaling and responses in Arabidopsis by independent research groups (see refs. in Supplemental Table S4). Hence, our experimental and literature validation approaches together provide evidence for 30 IPPs (29 interactors) among the 80 IPP interactome components (Supplemental Figs. S5 and S6).

DISCUSSION

Plant MAPKs regulate numerous physiological responses by interacting with upstream and downstream protein components (Rodriguez et al., 2010). This study utilized the Y2H screen system and established, to our knowledge, the first rice MAPK interactome network, which is composed of 74 NR protein interactors and 80 NR IPPs (Fig. 6). The mapped interactome is of high quality, as 30 IPPs (37.5%) were validated by experimental (in vivo and in vitro) and literature evidence (Supplemental Figs. S5 and S6); however, the data do not necessarily provide an accurate estimate of the error in our interaction map. Large proportions of the IPPs in the interactome are

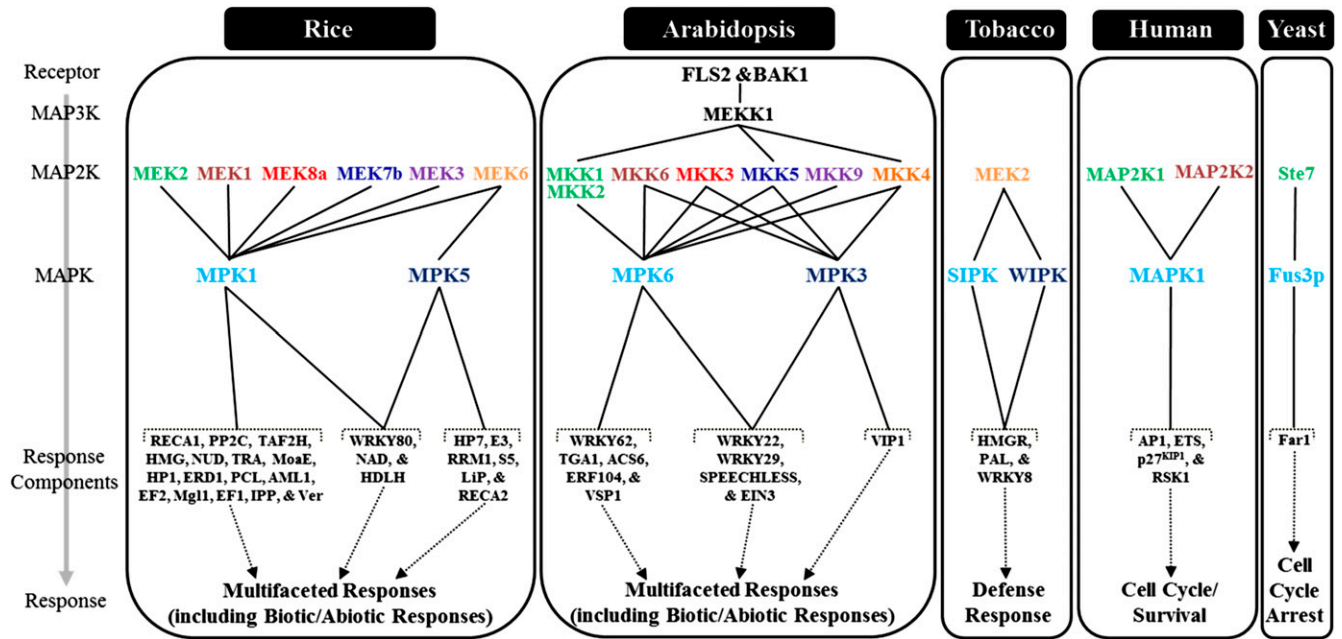


Figure 7. OsMPK1- and OsMPK5-mediated responses in organisms. The orthologs of OsMPK1 and OsMPK5 in Arabidopsis, tobacco, human, and yeast are shown, along with their interacting components, leading to different responses. Orthologous proteins are shown in the same colors. Some of the interacting components exhibited strong interactions as per the assay system used. [See online article for color version of this figure.]

novel in rice (91.2%) and in plants (73.7%), as shown (Supplemental Tables S3 and S4). Functional dissection of the novel MAPK interactors and their effect on the interactome (Fig. 7) will help to reveal as yet unknown biological roles and MAPK pathways in rice. Nevertheless, functional classification of the interactome components into 34 categories strengthens the evidence of the possible involvement of rice MAPKs in various physiological responses and expands our knowledge of rice at the systems level. Furthermore, it is likely that diverse physiological responses in rice seedlings are primarily controlled by a few MAPKs (Fig. 6). There are several possible reasons for the absence of IPPs for MAPKs other than OsMPK1, OsMPK5, OsMPK6, and OsMPK8. One possible explanation is the expression of these MAPKs and/or their interactors at very low levels in the rice seedlings that were used to prepare the cDNA library we screened.

In the rice interactome network, OsMPK1's interactors account for 51.2% of the mapped MAPK interaction network (Supplemental Table S3; Supplemental Fig. S7). The Arabidopsis OsMPK1 ortholog AtMAPK6 was previously shown to have about 40% more *in vitro* targets than all other MAPKs (Popescu et al., 2009). OsMPK1 also interacted with six of the eight predicted MAP2Ks in rice (Fig. 7; Agrawal et al., 2003b; Hamel et al., 2006; Reyna and Yang, 2006; Rao et al., 2010). Similarly, AtMAPK6 is likely to interact with seven MAP2Ks (Fig. 7). These large-scale studies suggest the central importance of OsMPK1 and AtMAPK6 in rice and Arabidopsis, respectively. Indeed, OsMPK1 and its orthologs (such as SIPK in tobacco and AtMAPK6) have been extensively studied in plants and are proposed to be central components regulating multiple physiological responses, including responses to stress (biotic and abiotic), as well as plant growth and development (Samuel et al., 2000; Ichimura et al., 2002; Nakagami et al., 2005). OsMPK1-mediated multifaceted responses appear to be conserved across Arabidopsis, tobacco, human, and yeast (Fig. 7). The compilation of reported experimental data (Fig. 7) reflects the fact that the upstream MAP2K regulators of OsMPK1 and its orthologs are likely to be more strongly conserved across organisms than their downstream effectors. The constructed rice MAPK network will provide a basic framework for better elucidating how OsMPK1 regulates multiple rice responses in time and space by interacting with multiple components. Follow-up *in vivo* experiments are essential to evaluate their physiological relevance.

In conclusion, this discovery process has provided a high-quality mapped MAPK interaction network as a rich data resource for (1) defining the complexities of MAPK networks controlling cellular physiology and responses and (2) creating a nearly complete rice MAPK interactome by applying Y2H and other parallel techniques to different rice tissues/organs during growth and development and under different biotic and abiotic stress conditions.

MATERIALS AND METHODS

Rice cDNA Library Construction

A rice (*Oryza sativa*) cDNA library was constructed from 3-week-old seedlings of *japonica* 'Dongjin.' Leaf tissue was used to extract total RNA by Tri-Reagent according to the manufacturers' protocol (catalog no. TR 118; Molecular Research Center). Two milligrams of mRNA was purified using the Oligo(dT)-Cellulose Type 7 mRNA purification kit as per the manufacturers' protocol (catalog no. 27-5543-02; Amersham Biosciences). Four micrograms of purified mRNA was used to construct a rice cDNA library with the CloneMiner cDNA Library construction kit as per the manufacturers' protocol (catalog no. 18249-029; Invitrogen). The titer of the library was approximately 2.9×10^6 colony-forming units μg^{-1} , with the insert size in the range of 0.5 to 2 kb.

Y2H Screen

The Y2H screen vectors (pDONR201, pDEST32, and pDEST22) were from Invitrogen. The rice cDNA clones were obtained from the Rice Genome Resource Center. The gene-specific primer pairs used in this study are listed in Supplemental Table S5. In the first stage of the Y2H screen, the full-length open reading frames of 53 rice MAPK-related proteins (MAP2Ks, MAPKs, TFs, and DRPs) were subcloned into the pDONR201 (donor) vector using the Gateway system (ProQuest Two-Hybrid System; Invitrogen). The open reading frame for each resulting "entry" clone was then integrated into both pDEST32 (DNA-binding [DB] domain) and pDEST22 (AD domain) Gateway-compatible "destination" vectors by a homologous recombination system (ProQuest Two-Hybrid System; Invitrogen). AH109 (Clontech) yeast cells were transformed with a total of 2,528 possible combinations (Supplemental Fig. S1) of DB and AD destination vectors to assess GAL4-based PPIs. Cells were grown on SC-LT selection plates (6.7 g L yeast nitrogen base without amino acids, 0.64 g L⁻¹ SC-LT, 20 g L⁻¹ agar, and 20 g L⁻¹ Glc) at 30°C for 4 d. Individual colonies were picked from the plates and cultured in 1 mL of SC-LT broth at 30°C overnight. The cultured cells were diluted to an optical density at 600 nm of 0.2 with distilled water and were spotted on SC-LTH selection plates (6.7 g L⁻¹ yeast nitrogen base without amino acids, 0.62 g L⁻¹ SC-LTH, 20 g L⁻¹ agar, 20 g L⁻¹ Glc, and 5 mm 3-AT) and incubated at 30°C for a maximum of 6 d. If cell growth was observed within 4 d, the interactors the cells harbored were deemed to be strong interacting protein pairs.

To perform Y2H genome-wide screening in rice, pDONR222 vectors carrying a rice leaf cDNA library from 3-week-old seedlings (cv Dongjin) were integrated into pDEST22 vector (prey). Nine MAPKs and MAP2Ks in pDEST32 were used as bait proteins. MaV203 (Invitrogen) yeast cells transformed with bait and prey vectors were spread on SC-LTH selection plates containing 55 mm 3-AT and grown at 30°C for 7 d. The concentration of 3-AT used was found to be sufficient to prevent autoactivation, as cells containing bait did not exhibit growth. The average transformation efficiency was 2.9×10^6 colony-forming units μg^{-1} . Individual colonies that appeared until 7 d were further streaked on SC-LT plates and grown at 30°C for 3 d. Each colony was then cultured in 1 mL of SC-LT broth at 30°C overnight. Diluted cultured cells (optical density at 600 nm = 0.2) were spotted on selection plates containing (1) SC-LTH with 0, 10, 25, 50, 75, or 100 mm 3-AT; (2) SC-LT; (3) SC-LTU; (4) SC-LT with 0.2% (v/v) 5-FOA; and (5) yeast extract peptone dextrose (YPD). Plates were incubated at 30°C for 5 d with the exception of the YPD plates (1 d). A β -galactosidase assay (Invitrogen) was carried out according to the supplier's protocol. Cells that showed growth within 4 d on SC-LTH, SC-LT, and SC-LTU, but not on SC-LT + 5-FOA, and a blue color on YPD within 48 h were deemed to harbor strong IPPs. Cells that showed growth on SC-LT and SC-LT + 5-FOA, low or no growth on SC-LTH or SC-LTU, and a light blue color or no color change on YPD over the course of 4 d or longer were deemed to harbor weak IPPs. A retransformation assay (Invitrogen) was also performed according to the supplier's protocol to eliminate false-positive PPIs. Isolated positive plasmids were subjected to nucleotide sequence analyses to confirm gene identities (Macrogen).

In Vivo Co-IP Assays

The full-length cDNAs were amplified using primers (Supplemental Table S5) and cloned into pDONR201 (donor) vector using the Gateway system (Invitrogen). The cDNA from the entry clone (pDONR201) is recombined to Co-IP vectors by the Gateway system (Invitrogen). Nucleotide sequences for each generated clone were confirmed by sequencing

(MacroGen). The constructed vectors pGWB18 (bait)/pGWB15 (prey) and pGWB9 (bait)/pGWB18 (prey) containing N-terminal Myc (pGWB18), HA (pGWB15), and His (pGWB9) tags were used for in vivo Co-IP (Nakagawa et al., 2007). For all vector pairs, a transient expression assay was performed by infiltrating tobacco (*Nicotiana benthamiana*) leaves with *Agrobacterium tumefaciens* cells (strain C58C1 pCH32) harboring bait, prey, and p19 silencing vectors (Walter et al., 2004; Kim et al., 2009b). Total protein was extracted from infiltrated and noninfiltrated leaves as described previously with slight modifications (Kim et al., 2009b). Prepared proteins (0.5 mg) in 20 μ L of protein A-Sepharose beads (Amersham Biosciences) were incubated at 4°C for 2 h with gentle shaking. Primary antibodies precoupled to protein A-Sepharose beads were then added, and the proteins were incubated at 4°C for a further 2 h. The beads were washed extensively with 1 \times phosphate-buffered saline. 2 \times SDS sample buffer (25 μ L) was added to the washed beads, and the microfuge tubes were incubated in boiling water for 5 min. The clear supernatant was subjected to 12% SDS-PAGE followed by immunoblot analysis. Anti-His (catalog no. SC-803; Santa Cruz Biotechnology), anti-Myc (catalog no. SC-40; Santa Cruz Biotechnology), and anti-HA (catalog no. A190-108A; Bethyl Laboratories) antibodies were used for immunoprecipitation and immunoblotting analyses according to the manufacturers' protocols. All of the above antibodies were used at 1:500 dilution.

In Vitro GST Pull-Down Assays

The protein expression vectors used were pRSET A (Invitrogen) and pGEX4T-1 (Amersham Biosciences). Full-length cDNAs were subcloned into the expression vectors pGEX4T-1 and pRSET A downstream of an N-terminal GST and His tag, respectively, using primers (Supplemental Table S5). Expression of recombinant proteins in *Escherichia coli* (BL21) was induced by adding 1 mM isopropyl-1-thio- β -D-galactopyranoside at 37°C for 6 h (with the exception of OsMPK8, whose expression was induced by incubating at 30°C for 6 h). Proteins were purified on Glutathione-Sepharose 4B (Amersham Biosciences) and nickel-nitrilotriacetic acid agarose chelating agarose CL-6B affinity resin (Peptron) according to the suppliers' instructions. Protein expression was checked by loading protein onto 12% SDS-polyacrylamide gels and staining with Coomassie Brilliant Blue. Eluted proteins were then concentrated using Ultracel 30K and 10K devices (Millipore). Pull-down assays were carried out according to a standard protocol (Kim et al., 2009b). Briefly, recombinant His fusion protein (bait) was precleared with Glutathione-Sepharose 4B beads (Amersham Biosciences) and incubated with GST or GST fusion protein (prey) bound to Glutathione-Sepharose 4B beads for 2 h at 4°C. After 2 h of incubation at 4°C, the beads were washed four times for 10 min at 4°C with phosphate-buffered saline. Proteins bound to the bead were eluted with 2 \times SDS sample buffer (25 μ L), separated by 12% SDS-PAGE, and processed for immunoblotting using anti-His antibody (1:500 dilution).

BiFC and Subcellular Localization

Full-length cDNAs for the bait and prey IPPs were subcloned adjacent to N- and C-terminal YFP fragments into the BiFC plasmids pUC-SPYNE and pUC-SPYCE, respectively, using primers (Supplemental Table S5). YFP fluorescence is detected if the expressed bait and prey proteins interact in vivo (Walter et al., 2004).

Rice leaf sheaths were prepared from 4-week-old seedlings and cut into approximately 10-cm-long strips. Twelve strips were placed side by side on a one-half-strength Murashige and Skoog plate for transformation by biolistic bombardment. DNA preparation and biolistic bombardment (Biolistic-PDS-1000/He Particle Delivery System; Bio-Rad) were performed as described previously (Lee et al., 2008b). Onion (*Allium cepa*) tissues were also prepared as described previously (Lee et al., 2008b). YFP fluorescence in transformed onion and sheath tissues was detected at 12 to 24 and 24 to 48 h post bombardment, respectively, using a TCS SP5 confocal laser microscope (Leica). Onion and rice cells were placed on a slide and visualized with $\times 10$ and $\times 60$ objective lenses, respectively, using an excitation wavelength of 514 nm (argon laser) and an emission wavelength of 520 to 560 nm.

The onion system was used for subcellular localization of the identified interactors as described previously (Lee et al., 2008b).

In Vitro Kinase Assays

MAPKs and MAP2Ks were expressed in *E. coli* (BL21) as fusion proteins with N-terminal His and GST tags, respectively. A kinase assay was performed as

described previously (Kim et al., 2009a). Briefly, 2 μ g of recombinant purified protein in 25 μ L of kinase buffer (25 mM Tris-HCl [pH 7.5], 0.2 mM EDTA, 5 mM MgCl₂, 4 mM 2-mercaptoethanol, 1 mM phenylmethylsulfonyl fluoride, 0.1 mM Na₃VO₄, 10 mM NaF, and 10 mM β -glycerophosphate) was mixed with MBP (2 μ g; artificial substrate, Invitrogen), 0.1 mM [γ -³²P]ATP (5,000 cpm pmol⁻¹), and 50 μ M ATP and incubated at 30°C for 30 min. The reaction was terminated by adding 25 μ L of 2 \times SDS buffer to the reaction mixture and boiling it for 5 min. The protein sample was then subjected to 12% SDS-PAGE. Gels were then stained with Coomassie Brilliant Blue and analyzed by autoradiography. For cophosphorylation kinase assays, the bait and prey interacting proteins were mixed together in equal amounts.

Literature Validation of Protein Interaction Sets

To validate the rice MAPK interactome, we performed comparative studies of identified protein interaction pairs with interlogs (literature-confirmed ortholog protein interaction pairs) in human, the yeast *Saccharomyces cerevisiae*, *Arabidopsis* (*Arabidopsis thaliana*), and tobacco with the National Center for Biotechnology Information search engine (<http://www.ncbi.nlm.nih.gov/>). Comparative studies were performed on the basis of not only the Y2H assay but also involvement and regulation in the same signaling pathways and the results of phosphorylation assays, in vitro interaction assays, and in silico analysis.

Sequence data from this article can be found in the GenBank/EMBL/COMB and TIGR data libraries under accession numbers given in Supplemental Tables S1 and S3.

Supplemental Data

The following materials are available in the online version of this article.

Supplemental Figure S1. A total of 2,528 possible combinatorial cross-Y2H interactions for 53 proteins.

Supplemental Figure S2. The identified MAPK interactors belong to 34 functional categories.

Supplemental Figure S3. Visualization of protein-protein interactions in onion epidermal cells by BiFC.

Supplemental Figure S4. In vitro kinase assay of individual and interacting MAPK proteins.

Supplemental Figure S5. Literature validation of 21 IPPs across rice, *Arabidopsis*, yeast, and human.

Supplemental Figure S6. Summary of the rice MAPK interactome identified by the Y2H screen.

Supplemental Figure S7. The OsMPK1 interactome.

Supplemental Table S1. Rice proteins used as bait proteins (53 bait proteins) and their corresponding interacting proteins (13 prey proteins), representing 13 NR interactors.

Supplemental Table S2. Summary of Y2H library screening.

Supplemental Table S3. The 80 rice IPPs identified by the Y2H rice cDNA library screen, representing a total of 74 NR interactors.

Supplemental Table S4. Literature validation of 21 interacting protein pairs, representing 24 NR interactors.

Supplemental Table S5. Primers used in this study.

Received May 15, 2012; accepted July 8, 2012; published July 11, 2012.

LITERATURE CITED

- Agrawal GK, Agrawal SK, Shibato J, Iwahashi H, Rakwal R (2003a) Novel rice MAP kinases *OsMSRMK3* and *OsWJUMK1* involved in encountering diverse environmental stresses and developmental regulation. *Biochem Biophys Res Commun* **300**: 775–783
- Agrawal GK, Iwahashi H, Rakwal R (2003b) Rice MAPKs. *Biochem Biophys Res Commun* **302**: 171–180
- Agrawal GK, Rakwal R (2006) Rice proteomics: a cornerstone for cereal food crop proteomes. *Mass Spectrom Rev* **25**: 1–53

- Agrawal GK, Rakwal R (2011) Rice proteomics: a move toward expanded proteome coverage to comparative and functional proteomics uncovers the mysteries of rice and plant biology. *Proteomics* **11**: 1630–1649
- Ahlfors R, Macioszek V, Rudd J, Brosché M, Schlichting R, Scheel D, Kangasjärvi J (2004) Stress hormone-independent activation and nuclear translocation of mitogen-activated protein kinases in *Arabidopsis thaliana* during ozone exposure. *Plant J* **40**: 512–522
- Andreasson E, Ellis B (2010) Convergence and specificity in the *Arabidopsis* MAPK nexus. *Trends Plant Sci* **15**: 106–113
- Arabidopsis Interactome Mapping Consortium (2011) Evidence for network evolution in an Arabidopsis interactome map. *Science* **333**: 601–607
- Asai T, Tena G, Plotnikova J, Willmann MR, Chiu WL, Gomez-Gomez L, Boller T, Ausubel FM, Sheen J (2002) MAP kinase signalling cascade in Arabidopsis innate immunity. *Nature* **415**: 977–983
- Bardwell AJ, Flatauer LJ, Matsukuma K, Thorner J, Bardwell L (2001) A conserved docking site in MEKs mediates high-affinity binding to MAP kinases and cooperates with a scaffold protein to enhance signal transmission. *J Biol Chem* **276**: 10374–10386
- Bardwell L (2006) Mechanisms of MAPK signalling specificity. *Biochem Soc Trans* **34**: 837–841
- Bardwell L, Cook JG, Chang EC, Cairns BR, Thorner J (1996) Signaling in the yeast pheromone response pathway: specific and high-affinity interaction of the mitogen-activated protein (MAP) kinases Kss1 and Fus3 with the upstream MAP kinase kinase Ste7. *Mol Cell Biol* **16**: 3637–3650
- Blüthgen N, Legewie S (2008) Systems analysis of MAPK signal transduction. *Essays Biochem* **45**: 95–107
- Chang L, Karin M (2001) Mammalian MAP kinase signalling cascades. *Nature* **410**: 37–40
- Chen Z, Gibson TB, Robinson F, Silvestro L, Pearson G, Xu B, Wright A, Vanderbilt C, Cobb MH (2001) MAP kinases. *Chem Rev* **101**: 2449–2476
- Feilner T, Hultschig C, Lee J, Meyer S, Immink RGH, Koenig A, Possling A, Seitz H, Beveridge A, Scheel D, et al (2005) High throughput identification of potential Arabidopsis mitogen-activated protein kinase substrates. *Mol Cell Proteomics* **4**: 1558–1568
- Feuillet C, Leach JE, Rogers J, Schnable PS, Eversole K (2011) Crop genome sequencing: lessons and rationales. *Trends Plant Sci* **16**: 77–88
- Fiil BK, Petersen K, Petersen M, Mundy J (2009) Gene regulation by MAP kinase cascades. *Curr Opin Plant Biol* **12**: 615–621
- Gandhi TKB, Zhong J, Mathivanan S, Karthick L, Chandrika KN, Mohan SS, Sharma S, Pinkert S, Nagaraju S, Periaswamy B, et al (2006) Analysis of the human protein interactome and comparison with yeast, worm and fly interaction datasets. *Nat Genet* **38**: 285–293
- Gopalbhai K, Jansen G, Beauregard G, Whiteway M, Dumas F, Wu C, Meloche S (2003) Negative regulation of MAPKK by phosphorylation of a conserved serine residue equivalent to Ser212 of MEK1. *J Biol Chem* **278**: 8118–8125
- Hamel LP, Nicole MC, Sritubtim S, Morency MJ, Ellis M, Ehling J, Beaudoin N, Barbazuk B, Klessig D, Lee J, et al (2006) Ancient signals: comparative genomics of plant MAPK and MAPKK gene families. *Trends Plant Sci* **11**: 192–198
- Hu CD, Kerppola TK (2003) Simultaneous visualization of multiple protein interactions in living cells using multicolor fluorescence complementation analysis. *Nat Biotechnol* **21**: 539–545
- Ichimura K, Shinozaki K, Tena G, Sheen J, Henry Y, Champion A, Kreis M, Zhang S, Hirt H, Wilson C, et al (2002) Mitogen-activated protein kinase cascades in plants: a new nomenclature. *Trends Plant Sci* **7**: 301–308
- Karimi M, Inzé D, Depicker A (2002) Gateway vectors for Agrobacterium-mediated plant transformation. *Trends Plant Sci* **7**: 193–195
- Khokhlatchev AV, Canagarajah B, Wilsbacher J, Robinson M, Atkinson M, Goldsmith E, Cobb MH (1998) Phosphorylation of the MAP kinase ERK2 promotes its homodimerization and nuclear translocation. *Cell* **93**: 605–615
- Kim CY, Lee SH, Park HC, Bae CG, Cheong YH, Choi YJ, Han CD, Lee SY, Lim CO, Cho MJ (2000) Identification of rice blast fungal elicitor-responsive genes by differential display analysis. *Mol Plant Microbe Interact* **13**: 470–474
- Kim JA, Cho K, Singh R, Jung YH, Jeong SH, Kim SH, Lee JE, Cho YS, Agrawal GK, Rakwal R, et al (2009a) Rice *OsACDR1* (*Oryza sativa* accelerated cell death and resistance 1) is a potential positive regulator of fungal disease resistance. *Mol Cells* **28**: 431–439
- Kim JG, Li X, Roden JA, Taylor KW, Aakre CD, Su B, Lalonde S, Kirik A, Chen Y, Baranage G, et al (2009b) *Xanthomonas* T3S effector XopN suppresses PAMP-triggered immunity and interacts with a tomato atypical receptor-like kinase and TGT1. *Plant Cell* **21**: 1305–1323
- Kolch W, Calder M, Gilbert D (2005) When kinases meet mathematics: the systems biology of MAPK signalling. *FEBS Lett* **579**: 1891–1895
- Lee J, Rudd JJ, Macioszek VK, Scheel D (2004) Dynamic changes in the localization of MAPK cascade components controlling pathogenesis-related (PR) gene expression during innate immunity in parsley. *J Biol Chem* **279**: 22440–22448
- Lee JS, Huh KW, Bhargava A, Ellis BE (2008a) Comprehensive analysis of protein-protein interactions between Arabidopsis MAPKs and MAPK kinases helps define potential MAPK signalling modules. *Plant Signal Behav* **3**: 1037–1041
- Lee MO, Cho K, Kim SH, Jeong SH, Kim JA, Jung YH, Shim J, Shibato J, Rakwal R, Tamogami S, et al (2008b) Novel rice *OsSIPK* is a multiple stress responsive MAPK family member showing rhythmic expression at mRNA level. *Planta* **227**: 981–990
- Ligterink W, Kroj T, zur Nieden U, Hirt H, Scheel D (1997) Receptor-mediated activation of a MAP kinase in pathogen defense of plants. *Science* **276**: 2054–2057
- Morsy M, Gouthu S, Orchard S, Thorncroft D, Harper JE, Mittler R, Cushman JC (2008) Charting plant interactomes: possibilities and challenges. *Trends Plant Sci* **13**: 183–191
- Nakagami H, Pitzschke A, Hirt H (2005) Emerging MAP kinase pathways in plant stress signalling. *Trends Plant Sci* **10**: 339–346
- Nakagawa T, Kurose T, Hino T, Tanaka K, Kawamukai M, Niwa Y, Toyooka K, Matsuoka K, Jinbo T, Kimura T (2007) Development of series of Gateway binary vectors, pGWBs, for realizing efficient construction of fusion genes for plant transformation. *J Biosci Bioeng* **104**: 34–41
- Pitzschke A, Schikora A, Hirt H (2009) MAPK cascade signalling networks in plant defense. *Curr Opin Plant Biol* **12**: 421–426
- Popescu SC, Popescu GV, Bachan S, Zhang Z, Gerstein M, Snyder M, Dinesh-Kumar SP (2009) MAPK target networks in Arabidopsis thaliana revealed using functional protein microarrays. *Genes Dev* **23**: 80–92
- Rao KP, Richa T, Kumar K, Raghuram B, Sinha AK (2010) *In silico* analysis reveals 75 members of mitogen-activated protein kinase kinase gene family in rice. *DNA Res* **17**: 139–153
- Reyna NS, Yang Y (2006) Molecular analysis of the rice MAP kinase gene family in relation to *Magnaporthe grisea* infection. *Mol Plant Microbe Interact* **19**: 530–540
- Rodriguez MC, Petersen M, Mundy J (2010) Mitogen-activated protein kinase signaling in plants. *Annu Rev Plant Biol* **61**: 621–649
- Samaj J, Ovecka M, Hlavacka A, Lecourieux F, Meskiene I, Lichtscheid I, Lenart P, Salaj J, Volkmann D, Bögre L, et al (2002) Involvement of the mitogen-activated protein kinase SIMK in regulation of root hair tip growth. *EMBO J* **21**: 3296–3306
- Samuel MA, Miles GP, Ellis BE (2000) Ozone treatment rapidly activates MAP kinase signalling in plants. *Plant J* **22**: 367–376
- Shaffer KL, Sharma A, Snapp EL, Hegde RS (2005) Regulation of protein compartmentalization expands the diversity of protein function. *Dev Cell* **9**: 545–554
- Sibéril Y, Doireau P, Gantet P (2001) Plant bZIP G-box binding factors: modular structure and activation mechanisms. *Eur J Biochem* **268**: 5655–5666
- Walter M, Chaban C, Schütze K, Batistic O, Weckermann K, Näke C, Blazevic D, Grefen C, Schumacher K, Oecking C, et al (2004) Visualization of protein interactions in living plant cells using bimolecular fluorescence complementation. *Plant J* **40**: 428–438
- Widmann C, Gibson S, Jarpe MB, Johnson GL (1999) Mitogen-activated protein kinase: conservation of a three-kinase module from yeast to human. *Physiol Rev* **79**: 143–180
- Xing T, Malik K, Martin T, Miki BL (2001) Activation of tomato PR and wound-related genes by a mutagenized tomato MAP kinase kinase through divergent pathways. *Plant Mol Biol* **46**: 109–120
- Yang KY, Liu Y, Zhang S (2001) Activation of a mitogen-activated protein kinase pathway is involved in disease resistance in tobacco. *Proc Natl Acad Sci USA* **98**: 741–746